Available online at www.sciencedirect.com
ScienceDirect
Journal of Sound and Vibration 311 (2008) 1420–1430
JOURNAL OF SOUND AND VIBRATION
www.elsevier.com/locate/jsvi

Short Communication

A continuous-mass TMM for free vibration analysis of a non-uniform beam with various boundary conditions and carrying multiple concentrated elements

Jong-Shyong Wu*, Chin-Tzu Chen

Department of System and Naval Mechatronic Engineering, National Cheng-Kung University, Tainan, Taiwan 701, Republic of China

Received 12 January 2007; received in revised form 26 September 2007; accepted 28 September 2007
Available online 5 November 2007

Abstract

This paper presents a modified continuous-mass (model) transfer matrix method (CTMM) to determine the natural frequencies and associated mode shapes of a uniform or non-uniform beam with various classical (or non-classical) boundary conditions (BCs) and carrying multiple sets of concentrated elements with each set consisting of a point mass (with eccentricity and rotary inertia), a translational spring and a rotational spring. To this end, a continuous non-uniform free–free beam is subdivided into several uniform beam segments (each having distributed mass) and any two adjacent beam segments are connected by a node at which various concentrated elements being attached. Next, the transfer matrix for the integration constants of arbitrary two adjacent beam segments joined at an intermediate node is derived, and then the characteristic equation of the entire vibrating system is derived by combining all transfer matrices for all intermediate nodes and considering the BCs of the entire free–free beam. It has been found that, based on the foregoing formulation for a non-uniform free–free beam, one may easily obtain the mathematical model for a uniform or non-uniform beam with various BCs and carrying various concentrated elements by only adjusting the magnitudes of cross-sectional area and length of each beam segment and those of the concentrated elements (such as the lumped mass m_i with eccentricity e_i and rotary inertia J_i, the translational spring with stiffness $k_{t,i}$ and/or the rotational spring with stiffness $k_{r,i}$) attached to each node. The reliability of the presented results has been confirmed by comparing them with those of the existing literature or the conventional finite element method (FEM) and good agreement is achieved.
© 2007 Elsevier Ltd. All rights reserved.

1. Introduction

Since the dynamic characteristics of some structural systems may be predicted by using a beam carrying single or multiple concentrated elements, the literature concerned is plenty. For the free vibration analysis of beams with various attachments, the lumped-mass (model) transfer matrix method (LTMM) is one of the most popular approaches in early years [1–10]. Later, various classical analytical methods are presented to solve the similar problems [11–18]. One of the drawbacks of LTMM is the requirement of finer beam segments to achieve better accuracy of its numerical results and that of the classical analytical methods is not

*Corresponding author.
E-mail address: jswu@mail.ncku.edu.tw (J.-S. Wu).

0022-460X/$ - see front matter © 2007 Elsevier Ltd. All rights reserved.
doi:10.1016/j.jsv.2007.09.048

available for the more complicated problems. To improve the drawbacks of the last existing approaches, some researchers devoted themselves to the study of continuous-mass (model) transfer matrix method (CTMM) [19–24].

From reviews of the existing literature [1–23], one finds that the information regarding the free vibration analysis of a non-uniform beam with various boundary conditions (BCs) and carrying multiple sets of various concentrated elements is rare, thus, the purpose of this paper is to extend the theories of Refs. [24,25] to the presented modified CTMM. In which, the transfer matrix method (TMM) based on the lumped-mass model in Ref. [25] is extended to the TMM based on the continuous-mass model in this paper. To achieve the last goal, a continuous non-uniform *free–free* beam is subdivided into several uniform beam segments (each having distributed mass) and any two adjacent beam segments are connected by a node at which various concentrated elements being attached. Next, the transfer matrix for the integration constants of arbitrary two adjacent beam segments joined at an intermediate node i is derived, and then the characteristic equation of the entire vibrating system is obtained by combining the transfer matrices for all intermediate nodes and considering the BCs of the entire *free–free* beam. It has been found that, based on the foregoing formulation for a non-uniform *free–free* beam, one may easily obtain the mathematical model for a uniform or non-uniform beam with various BCs and carrying various concentrated elements by only adjusting the magnitudes of cross-sectional area and length of each beam segment and those of the concentrated elements (such as the lumped mass m_i with eccentricity e_i and rotary inertia J_i, the translational spring with stiffness $k_{t,i}$ and/or the rotational spring with stiffness $k_{r,i}$) attached to each node i. Besides, the *continuous-mass* instead of the *lumped-mass* model is used to the formulation of problem, the solution of the modified CTMM will be very close to the exact one even if the entire beam is subdivided into only a few beam segments. For this reason, the computer memory and the CPU time required by modified CTMM will be much less than those required by the conventional finite element method (FEM) for achieving the same accuracy.

2. Equation of motion and displacement function

The sketch for the non-uniform free–free beam studied in this paper is shown in Fig. 1. It is composed of n uniform beam segments (denoted by (1), (2), …, (i−1), (i), (i+1), …, (n)) separated by n−1 nodes (denoted by 2, 3, …, i−1, i, i+1, …, n) and carrying a lumped mass m_i (with eccentricity e_i and rotary inertia J_i), a translational spring with stiffness $k_{t,i}$ and a rotational spring with stiffness $k_{r,i}$ at each node i, $i = 1 \sim n+1$. For the ith beam segment (cf. Fig. 1), its equation of motion for free vibration is given by

$$E_i I_i \frac{\partial^4 y_i(x,t)}{\partial x^4} + \rho_i A_i \frac{\partial^2 y_i(x,t)}{\partial t^2} = 0 \quad (\text{for } x_i \le x \le x_{i+1}), \tag{1}$$

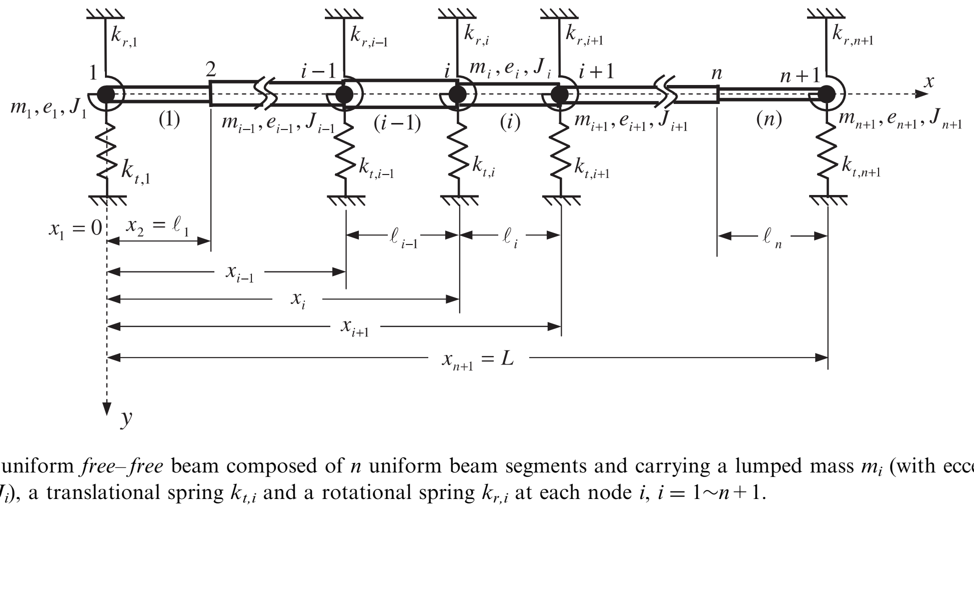

Fig. 1. A non-uniform *free–free* beam composed of n uniform beam segments and carrying a lumped mass m_i (with eccentricity e_i and rotary inertia J_i), a translational spring $k_{t,i}$ and a rotational spring $k_{r,i}$ at each node i, $i = 1 \sim n+1$.

where ρ_i, E_i and A_i are mass density, Young's modulus and cross-sectional area of the ith beam segment, respectively, I_i is moment of inertia of area A_i, while $y_i(x, t)$ is transverse displacement function of the ith beam segment at axial coordinate x and time t.

According to the theory of separation variables, one sets

$$y_i(x,t) = Y_i(x)\mathrm{e}^{\mathrm{i}\omega t}, \tag{2}$$

where $Y_i(x)$ is amplitude function of the ith beam segment and ω is the natural frequency of the entire non-uniform beam.

Substituting Eq. (2) into Eq. (1), one has

$$Y_i''''(x) - \beta_i^4 Y_i(x) = 0 \quad (\text{for } x_i \le x \le x_{i+1}) \tag{3}$$

with

$$\beta_i^4 = \omega^2\left(\frac{\rho_i A_i}{E_i I_i}\right), \tag{4}$$

where the primes ($'$) denote differentiations with respect to the axial coordinate x.

The solution of Eq. (3) takes the form

$$Y_i(x) = A_i \cos \beta_i x + B_i \sin \beta_i x + C_i \cosh \beta_i x + D_i \sinh \beta_i x \quad (\text{for } x_i \le x \le x_{i+1}). \tag{5}$$

3. Natural frequencies and mode shapes of the entire beam

The continuity of displacements and slopes, and the equilibrium of shear forces and bending moments for the two beam segments, (i–1) and (i), joined at the intermediate node i (cf. Fig. 1) require that

$$Y_{i-1}(x_i) = Y_i(x_i), \tag{6a}$$

$$Y'_{i-1}(x_i) = Y'_i(x_i), \tag{6b}$$

$$E_{i-1}I_{i-1}Y'''_{i-1}(x_i) = E_iI_iY'''_i(x_i) - m_i\omega^2 Y_i(x_i) + k_{t,i}Y_i(x_i) - m_ie_i\omega^2 Y'_i(x_i), \tag{6c}$$

$$E_{i-1}I_{i-1}Y''_{i-1}(x_i) = E_iI_iY''_i(x_i) - k_{r,i}Y'_i(x_i) + (J_i + m_ie_i^2)\omega^2 Y'_i(x_i) + m_ie_i\omega^2 Y_i(x_i). \tag{6d}$$

Note that the effects due to rotary inertia J_i and eccentricity e_i of the lumped mass m_i are not considered in Ref. [24].

The non-uniform beam shown in Fig. 1 is a free–free (F–F) beam, thus, the shear forces and bending moments at its two ends, nodes 1 and $n+1$, must be equal to zero, i.e.,

$$E_1I_1Y'''_1(0) - m_1\omega^2 Y_1(0) + k_{t,1}Y_1(0) - m_1e_1\omega^2 Y'_1(0) = 0, \tag{7a}$$

$$E_1I_1Y''_1(0) - k_{r,1}Y'_1(0) + (J_1 + m_1e_1^2)\omega^2 Y'_1(0) + m_1e_1\omega^2 Y_1(0) = 0, \tag{7b}$$

$$E_nI_nY'''_n(L) + m_{n+1}\omega^2 Y_n(L) - k_{t,n+1}Y_n(L) + m_{n+1}e_{n+1}\omega^2 Y'_n(L) = 0, \tag{8a}$$

$$E_nI_nY''_n(L) + k_{r,n+1}Y'_n(L) - (J_{n+1} + m_{n+1}e_{n+1}^2)\omega^2 Y'_n(L) - m_{n+1}e_{n+1}\omega^2 Y_n(L) = 0. \tag{8b}$$

From Eqs. (5) and (6a)–(6d) one obtains

$$\begin{aligned} &A_{i-1}\cos\beta_{i-1}x_i + B_{i-1}\sin\beta_{i-1}x_i + C_{i-1}\cosh\beta_{i-1}x_i + D_{i-1}\sinh\beta_{i-1}x_i \\ &\quad = A_i\cos\beta_i x_i + B_i\sin\beta_i x_i + C_i\cosh\beta_i x_i + D_i\sinh\beta_i x_i, \end{aligned} \tag{9a}$$

$$\begin{aligned} &\beta_{i-1}(-A_{i-1}\sin\beta_{i-1}x_i + B_{i-1}\cos\beta_{i-1}x_i + C_{i-1}\sinh\beta_{i-1}x_i + D_{i-1}\cosh\beta_{i-1}x_i) \\ &\quad = \beta_i(-A_i\sin\beta_i x_i + B_i\cos\beta_i x_i + C_i\sinh\beta_i x_i + D_i\cosh\beta_i x_i), \end{aligned} \tag{9b}$$

$$\begin{aligned} &A_{i-1}\sin\beta_{i-1}x_i - B_{i-1}\cos\beta_{i-1}x_i + C_{i-1}\sinh\beta_{i-1}x_i + D_{i-1}\cosh\beta_{i-1}x_i \\ &\quad = (P_i\sin\beta_i x_i + R_i\cos\beta_i x)A_i + (-P_i\cos\beta_i x_i + R_i\sin\beta_i x)B_i \\ &\quad + (Q_i\sinh\beta_i x_i + R_i\cosh\beta_i x)C_i + (Q_i\cosh\beta_i x_i + R_i\sinh\beta_i x)D_i, \end{aligned} \tag{9c}$$

$$\begin{aligned} &-A_{i-1}\cos\beta_{i-1}x_i - B_{i-1}\sin\beta_{i-1}x_i + C_{i-1}\cosh\beta_{i-1}x_i + D_{i-1}\sinh\beta_{i-1}x_i \\ &\quad = A_i(-\bar{Q}_i\cos\beta_i x_i - \bar{R}_i\sin\beta_i x_i) + B_i(-\bar{Q}_i\sin\beta_i x_i + \bar{R}_i\cos\beta_i x_i) \\ &\quad + C_i(\bar{P}_i\cosh\beta_i x_i + \bar{R}_i\sinh\beta_i x_i) + D_i(\bar{P}_i\sinh\beta_i x_i + \bar{R}_i\cosh\beta_i x_i), \end{aligned} \tag{9d}$$

where

$$P_i = \frac{E_iI_i\beta_i^3 + m_ie_i\omega^2\beta_i}{E_{i-1}I_{i-1}\beta_{i-1}^3}, \quad Q_i = \frac{E_iI_i\beta_i^3 - m_ie_i\omega^2\beta_i}{E_{i-1}I_{i-1}\beta_{i-1}^3}, \quad R_i = \frac{k_{t,i} - m_i\omega^2}{E_{i-1}I_{i-1}\beta_{i-1}^3}, \tag{10a–c}$$

$$\bar{P}_i = \frac{E_iI_i\beta_i^2 + m_ie_i\omega^2}{E_{i-1}I_{i-1}\beta_{i-1}^2}, \quad \bar{Q}_i = \frac{E_iI_i\beta_i^2 - m_ie_i\omega^2}{E_{i-1}I_{i-1}\beta_{i-1}^2}, \quad \bar{R}_i = \frac{[(J_i + m_ie_i^2)\omega^2 - k_{r,i}]\beta_i}{E_{i-1}I_{i-1}\beta_{i-1}^2}. \tag{10d–f}$$

To write Eqs. (9a)–(9d) in matrix form, one has

$$[G]_{i-1}\{\delta\}_{i-1} = [H]_i\{\delta\}_i, \tag{11}$$

where

$$\{\delta\}_i = \{A_i \quad B_i \quad C_i \quad D_i\}, \quad \{\delta\}_{i-1} = \{A_{i-1} \quad B_{i-1} \quad C_{i-1} \quad D_{i-1}\}, \tag{12a,b}$$

$$[G]_{i-1} = \begin{bmatrix} \cos\theta_{i-1} & \sin\theta_{i-1} & \cosh\theta_{i-1} & \sinh\theta_{i-1} \\ -\beta_{i-1}\sin\theta_{i-1} & \beta_{i-1}\cos\theta_{i-1} & \beta_{i-1}\sinh\theta_{i-1} & \beta_{i-1}\cosh\theta_{i-1} \\ \sin\theta_{i-1} & -\cos\theta_{i-1} & \sinh\theta_{i-1} & \cosh\theta_{i-1} \\ -\cos\theta_{i-1} & -\sin\theta_{i-1} & \cosh\theta_{i-1} & \sinh\theta_{i-1} \end{bmatrix}, \tag{13}$$

$$[H]_i = \begin{bmatrix} \cos\theta_i & \sin\theta_i & \cosh\theta_i & \sinh\theta_i \\ -\beta_i\sin\theta_i & \beta_i\cos\theta_i & \beta_i\sinh\theta_i & \beta_i\cosh\theta_i \\ P_i\sin\theta_i + R_i\cos\theta_i & -P_i\cos\theta_i + R_i\sin\theta_i & Q_i\sinh\theta_i + R_i\cosh\theta_i & Q_i\cosh\theta_i + R_i\sinh\theta_i \\ -\bar{Q}_i\cos\theta_i - \bar{R}_i\sin\theta_i & -\bar{Q}_i\sin\theta_i + \bar{R}_i\cos\theta_i & \bar{P}_i\cosh\theta_i + \bar{R}_i\sinh\theta_i & \bar{P}_i\sinh\theta_i + \bar{R}_i\cosh\theta_i \end{bmatrix} \tag{14}$$

with

$$\theta_i = \beta_i x_i, \tag{15}$$

$$\theta_{i-1} = \beta_{i-1}x_i. \tag{16}$$

From Eq. (11) one obtains

$$\{\delta\}_i = [H]_i^{-1}[G]_{i-1}\{\delta\}_{i-1} = [T]_{i-1}\{\delta\}_{i-1}, \tag{17}$$

where

$$[T]_{i-1} = [H]_i^{-1}[G]_{i-1}, \tag{18}$$

which represents the transfer matrix between the integration constants for beam segment (i), $\{\delta\}_i$, and those for beam segment (i–1), $\{\delta\}_{i-1}$, joined at the intermediate node i.

From Eq. (17), one has

$$\{\delta\}_n = [T]_{n-1}\{\delta\}_{n-1} = [T]_{n-1}[T]_{n-2}\{\delta\}_{n-2} = \ldots = [T]_{n-1}[T]_{n-2}\ldots[T]_2[T]_1\{\delta\}_1 = [T]\{\delta\}_1, \tag{19}$$

where

$$[T] = [T]_{n-1}[T]_{n-2}\ldots[T]_2[T]_1 = \begin{bmatrix} T_{11} & T_{12} & T_{13} & T_{14} \\ T_{21} & T_{22} & T_{23} & T_{24} \\ T_{31} & T_{32} & T_{33} & T_{34} \\ T_{41} & T_{42} & T_{43} & T_{44} \end{bmatrix}. \tag{20}$$

It is noted that the symbols { } and [ ] denote the column vector and square matrix, respectively, and $\{\ldots\}\equiv[\ldots]^{\mathrm{T}}$ with $[\ldots]^{\mathrm{T}}$ denoting the transpose of a row matrix.

For the beam segment at *left* end of the beam with $x_1 = 0$ (cf. Fig. 1), from Eqs. (5) and (7a), one obtains

$$S_{11}A_1 + S_{12}B_1 + S_{13}C_1 + S_{14}D_1 = 0, \tag{21a}$$

$$S_{21}A_1 + S_{22}B_1 + S_{23}C_1 + S_{24}D_1 = 0, \tag{21b}$$

where

$$S_{11} = k_{t,1} - m_1\omega^2, \quad S_{12} = -(E_1I_1\beta_1^3 + m_1e_1\omega^2\beta_1), \tag{22a,b}$$

$$S_{13} = k_{t,1} - m_1\omega^2, \quad S_{14} = E_1I_1\beta_1^3 - m_1e_1\omega^2\beta_1, \tag{22c,d}$$

$$S_{21} = m_1e_1\omega^2 - E_1I_1\beta_1^2, \quad S_{22} = [(J_1 + m_1e_1^2)\omega^2 - k_{r,1}]\beta_1, \tag{23a,b}$$

$$S_{23} = m_1e_1\omega^2 + E_1I_1\beta_1^2, \quad S_{24} = [(J_1 + m_1e_1^2)\omega^2 - k_{r,1}]\beta_1. \tag{23c,d}$$

Similarly, for the beam segment at *right* end of the beam with $x_{n+1} = L$ (cf. Fig. 1), from Eqs. (5) and (8a), one has

$$U_{11}A_n + U_{12}B_n + U_{13}C_n + U_{14}D_n = 0, \tag{24a}$$

$$U_{21}A_n + U_{22}B_n + U_{23}C_n + U_{24}D_4 = 0, \tag{24b}$$

where

$$U_{11} = (E_nI_n\beta_n^3 - m_{n+1}e_{n+1}\omega^2\beta_n)\sin\beta_nL - (k_{t,n+1} - m_{n+1}\omega^2)\cos\beta_nL, \tag{25a}$$

$$U_{12} = -(E_nI_n\beta_n^3 - m_{n+1}e_{n+1}\omega^2\beta_n)\cos\beta_nL - (k_{t,n+1} - m_{n+1}\omega^2)\sin\beta_nL, \tag{25b}$$

$$U_{13} = (E_nI_n\beta_n^3 + m_{n+1}e_{n+1}\omega^2\beta_n)\sinh\beta_nL - (k_{t,n+1} - m_{n+1}\omega^2)\cosh\beta_nL, \tag{25c}$$

$$U_{14} = (E_nI_n\beta_n^3 + m_{n+1}e_{n+1}\omega^2\beta_n)\cosh\beta_nL - (k_{t,n+1} - m_{n+1}\omega^2)\sinh\beta_nL, \tag{25d}$$

$$U_{21} = -(E_nI_n\beta_n^2 + m_{n+1}e_{n+1}\omega^2)\cos\beta_nL + [(J_{n+1} + m_{n+1}e_{n+1}^2)\omega^2 - k_{r,n+1}]\beta_n\sin\beta_nL, \tag{26a}$$

$$U_{22} = -(E_nI_n\beta_n^2 + m_{n+1}e_{n+1}\omega^2)\sin\beta_nL - [(J_{n+1} + m_{n+1}e_{n+1}^2)\omega^2 - k_{r,n+1}]\beta_n\cos\beta_nL \tag{26b}$$

$$U_{23} = (E_nI_n\beta_n^2 - m_{n+1}e_{n+1}\omega^2)\cosh\beta_nL - [(J_{n+1} + m_{n+1}e_{n+1}^2)\omega^2 - k_{r,n+1}]\beta_n\sinh\beta_nL, \tag{26c}$$

$$U_{24} = (E_nI_n\beta_n^2 - m_{n+1}e_{n+1}\omega^2)\sinh\beta_nL - [(J_{n+1} + m_{n+1}e_{n+1}^2)\omega^2 - k_{r,n+1}]\beta_n\cosh\beta_nL. \tag{26d}$$

To write the two equations for the *right-end* BCs given by Eqs. (24a,b) in matrix form, one obtains

$$[U]\{\delta\}_n = 0, \tag{27}$$

where

$$[U] = \begin{bmatrix} U_{11} & U_{12} & U_{13} & U_{14} \\ U_{21} & U_{22} & U_{23} & U_{24} \end{bmatrix}. \tag{28}$$

Introducing the overall transfer matrix $[T]$ defined by Eq. (19) into Eq. (27) gives

$$[U][T]\{\delta\}_1 = 0 \tag{29a}$$

or

$$[V]\{\delta\}_1 = 0, \tag{29b}$$

where

$$[V] = [U]_{2\times 4}[T]_{4\times 4}. \tag{30}$$

Combining the other two equations for the *left-end* BCs given by Eqs. (21a,b) with Eq. (29b), one obtains

$$[W]\{\delta\}_1 = 0 \tag{31}$$

with

$$[W] = \begin{bmatrix} S_{11} & S_{12} & S_{13} & S_{14} \\ S_{21} & S_{22} & S_{23} & S_{24} \\ V_{11} & V_{12} & V_{13} & V_{14} \\ V_{21} & V_{22} & V_{23} & V_{24} \end{bmatrix}. \tag{32}$$

Since Eq. (31) represents a set of simultaneous equations, non-trivial solution requires that its coefficient determinant is equal to zero, i.e.,

$$|W| = \begin{vmatrix} S_{11} & S_{12} & S_{13} & S_{14} \\ S_{21} & S_{22} & S_{23} & S_{24} \\ V_{11} & V_{12} & V_{13} & V_{14} \\ V_{21} & V_{22} & V_{23} & V_{24} \end{vmatrix} = 0. \tag{33}$$

Eq. (33) is the frequency equation, from which one may determine the natural frequencies ω_v ($v = 1, 2, 3, \ldots$) and corresponding to each natural frequency one may obtain the associated integrations $\{\delta\}_1 = \{A_1\ B_1\ C_1\ D_1\}$ from Eq. (31). Once the integration constants for the first beam segment, $\{\delta\}_1$, are determined, those of the other beam segments, $\{\delta\}_i$ ($i = 2,3, \ldots, n$), may obtained from Eq. (17), and substituting the integration constants for all beam segments, $\{\delta\}_i$ ($i = 1,2,3, \ldots, n$), into Eq. (5), one will determine the associated mode shape of the entire beam, $Y^{(v)}(x)$.

4. Numerical results and discussions

For convenience of comparisons, the dimensions and physical constants of the beams studied in this paper are taken to be the same as those of Ref. [25]: total length $L = 2.0\,\mathrm{m}$, diameter $d_1 = 0.03\,\mathrm{m}$, mass density $\rho_1 = 7850\,\mathrm{kg/m^3}$, Young's modulus $E_1 = 2.068 \times 10^{11}\,\mathrm{N/m^2}$, cross-sectional area $A_1 = \pi d_1^2/4 = 7.069 \times 10^{-4}\,\mathrm{m^2}$, area moment of inertia $I_1 = \pi d_1^4/64 = 3.976 \times 10^{-8}\,\mathrm{m^4}$, reference mass $\tilde{m} = \rho_1 A_1 L = 11.09833l\,\mathrm{kg}$, reference rotary inertia $\tilde{J} = \rho_1 A_1 L^3 = \tilde{m}L^2 = 44.39332\,\mathrm{kg\,m^2}$, reference rigidity $E_1 I_1 = 8.2224 \times 10^3\,\mathrm{N\,m^2}$, reference rotational spring constant $\tilde{k}_r = E_1 I_1/L = 4.1112 \times 10^3\,\mathrm{N\,m}$, reference translational spring constant $\tilde{k}_t = E_1 I_1/L^3 = 1.0278 \times 10^3\,\mathrm{N/m}$. In the foregoing expressions, the subscript 1 refers to *field* 1 (or *beam segment* 1).

4.1. A "stepped" beam carrying multiple sets of concentrated elements

The current stepped beam has two stepped changes in cross-sections with diameters of the stepped beam segments to be $d_1 = 0.03\,\mathrm{m}$, $d_2 = 0.04\,\mathrm{m}$ and $d_3 = 0.05\,\mathrm{m}$, as one may see from Fig. 2. Besides, the stepped beam carries three identical sets of concentrated elements. Each set of concentrated elements includes a lumped mass m_i (with eccentricity e_i and rotary inertia J_i), a translational spring (with stiffness constant $k_{t,i}$) and a rotational spring (with stiffness constant $k_{r,i}$). The magnitudes of the concentrated elements are: $m_i = \tilde{m} = 11.09833l\,\mathrm{kg}$, $e_i = 0.01L = 0.02\,\mathrm{m}$, $J_i = 0.1\tilde{J} = 4.439332\,\mathrm{kg\,m^2}$, $k_{t,i} = \tilde{k}_t = 1.0278 \times 10^3\,\mathrm{N/m}$ and

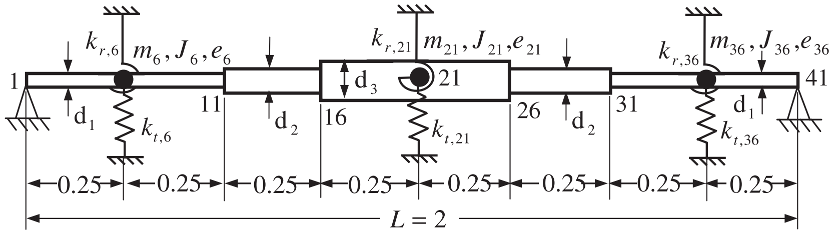

Fig. 2. A three-step P–P beam carrying three identical sets of concentrated elements located at $\xi_i = x_i/L = 0.125$, 0.5 and 0.875, respectively. The unit for all lengths in the figure is "meter" and the station numberings are for LTMM and FEM only.

Table 1
The lowest five natural frequencies, ω_v (v = 1–5), for the three-step beam (cf. Fig. 2) carrying three identical sets of concentrated elements located at $\xi_i = x_i/L = 0.125$, 0.5 and 0.875, respectively

Boundary conditions	Methods	Natural frequencies, ω_v (rad/s)				
		ω_1	ω_2	ω_3	ω_4	ω_5
P–P	LTMM	57.3317	108.1611	268.9405	281.6411	467.3322
	CTMM	57.3303	108.1652	268.9206	281.6431	467.0818
	FEM	57.3303	108.1651	268.9206	281.6434	467.3489
C–C	LTMM	97.0301	131.5889	293.7608	317.5620	751.8541
	CTMM	97.0273	131.5916	293.7228	317.5613	751.9225
	FEM	97.0273	131.5916	293.7228	317.5617	751.9331
C–F	LTMM	21.8981	79.1734	124.5587	307.1878	387.4394
	CTMM	21.8995	79.1755	124.5614	307.1629	387.4295
	FEM	21.8995	79.1755	124.5614	307.1629	387.4302
C–P	LTMM	73.3668	124.4120	270.6345	310.0435	468.4279
	CTMM	73.3654	124.4147	270.6195	310.0296	468.4319
	FEM	73.3654	124.4147	270.6195	310.0298	468.4508

Note: (i) $m_i = J_i = e_i = k_{t,i} = k_{r,i} = 0$ except those at $\xi_i = x_i/L = 0.125$, 0.5 and 0.875.
(ii) Total number of *beam segments* is $n = 40$ for LTMM and FEM, and $n = 8$ for CTMM.

$k_{r,i} = \tilde{k}_r = 4.1112 \times 10^3\,\mathrm{N\,m}$ ($i = 6$, 21, 36 for LTMM and FEM; $i = 2$, 5, 8 for CTMM), where i denotes the "station" numbering, and the total number of "beam segments" is $n = 40$ for LTMM and FEM and $n = 8$ for CTMM. The digits in Fig. 2 represent the numberings for the associated "stations" (for LTMM and FEM only), and the locations of the three sets of concentrated elements are: $\xi_I = x_i/L = 0.125$, 0.5 and 0.875, respectively. It is noted that the unit for all lengths in the figure is "meter".

Four classical boundary (supporting) conditions of the stepped beam are studied: pinned–pinned (P–P), clamped–clamped (C–C), clamped–free (C–F) and clamped–pinned (C–P). The lowest five natural frequencies of the stepped beam, ω_v (v = 1–5), obtained from LTMM, CTMM and FEM are listed in Table 1. Note that, in LTMM and CTMM, a pinned end is modeled by $k_t = 1.0 \times 10^{15}\,\mathrm{N/m}$ and $k_r = 0$; a clamped end by $k_t = 1.0 \times 10^{15}\,\mathrm{N/m}$ and $k_r = 1.0 \times 10^{15}\,\mathrm{N\,m}$; a free end by $k_t = k_r = 0$.

4.2. Influence of total number of beam segments (n) on solution convergence

Because the solution convergence of either LTMM or FEM has something to do with the problems tackled, two kinds of vibrating system are studied in this subsection: a uniform beam with one set of concentrated elements located at mid-length (cf. Fig. 3) and a three-step beam carrying three intermediate identical sets of concentrated elements (cf. Fig. 2).

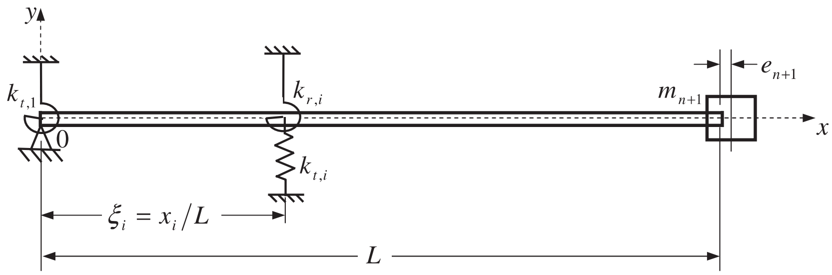

Fig. 3. A spring-hinged uniform beam carrying an eccentric tip mass.

4.2.1. A uniform spring-hinged beam with an eccentric tip mass and a set of in-span springs

For the uniform spring-hinged beam carrying an eccentric tip mass and a set of in-span springs as shown in Fig. 3, and with $k^*_{r,1} = k_{r,1}/\tilde{k}_r = 10^5$, $k^*_{r,i} = k_{r,i}/\tilde{k}_r = 10$, $k^*_{t,i} = k_{t,i}/\tilde{k}_t = 10$, $J^*_{n+1} = J_{n+1}/\tilde{J} = 0.1$, $e^*_{n+1} = e_{n+1}/L = 0.1$, $m^*_{n+1} = m_{n+1}/\tilde{m} = 5$ and $\xi_i = x_i/L = 0.5$, the influence of total number of beam segments (n) on accuracy of the lowest five natural frequencies, ω_v (v = 1–5), is shown in Table 2 and Fig. 4. Since the results of CTMM based on $n = 4$ are the same as those based on $n = 2$, as one may see from Table 2(a), the solution of CTMM for the current example is the exact one, the percentage errors (ε%) in the parentheses of Table 2(a) are determined from the formula: $\varepsilon = (\omega_{i,,X} - \omega_{i,\mathrm{CTMM}}) \times 100\%/\omega_{i,\mathrm{CTMM}}$ with $\omega_{i,X}$ denoting the ith natural frequency obtained from X method (X = LTMM or FEM). Based on the absolute values of ε, five figures showing the solution convergence versus total number of beam segments (n) are plotted in Figs. 4(a)–(e) for ω_1, ω_2, ω_3, ω_4 and ω_5, respectively. In which, the solid curves (—●—, —✚—, -▲-, —■— and —★—) are for the solution of LTMM and the dashed curves (---○---, ---✖---, ---△---, ---□--- and ---☆---) are for that of FEM.

From Table 2(a) one sees that, for the case of $n = 2$, LTMM can only determine the second rough natural frequency ($\omega_2 = 73.2035 \approx 71.2678$ rad/s) but FEM cannot determine any reasonable natural frequencies (because $\omega_1 = 22.4584 \gg 11.2087$ rad/sand $\omega_2 = 127.3449 \gg 71.2678$ rad/s). However, for the case of $n = 4$, FEM can determine the lowest "five" reasonable natural frequencies but LTMM can determine only the lowest "four". For the last reason, the minimum number of beam segments for the solution convergence graphs shown in Figs. 4(a)–(e) is $n_{\min} = 6$. For the case of $n = 14$, the maximum percentage error for the lowest five natural frequencies is $\varepsilon_{\max} = 0.040\%$ for ω_2 obtained from LTMM and $\varepsilon_{\max} = 0.026\%$ for ω_5 obtained from FEM as one may see from Table 2(a) and Fig. 4. Based on the foregoing discussions, one may say that one of the predominant advantages of CTMM superior to LTMM or FEM should be its capable of achieving accurate solution using only a few beam segments.

4.2.2. A three-step beam with three identical sets of concentrated elements in P–P BCs

For the three-step beam carrying three identical sets of concentrated elements with P–P BCs as shown in Fig. 2 and Case 1 of Table 1, the influence of total number of beam segments (n) on accuracy of the lowest five natural frequencies, ω_v (v = 1–5), is shown in Table 2(b). In Fig. 2, the entire beam has 4 stepped changes of cross-sections and 3 attaching points for the 3 identical sets of concentrated elements. For the last reason, the minimum number of beam segments for either LTMM, CTMM or FEM is eight ($n_{\min} = 8$) for the *stepped beam* shown in Fig. 2 instead of two ($n_{\min} = 2$) for CTMM for the *uniform beam* shown in Fig. 3. The percentage differences (ε%) between the lowest five natural frequencies obtained from LTMM (i.e., $\omega_{i,\mathrm{LTMM}}$, $i = 1-5$) and the corresponding ones obtained from CTMM (i.e., $\omega_{i,\mathrm{CTMM}}$, $i = 1-5$, with $n = n_{\min} = 8$) are shown in the parentheses in upper part of Table 2(b) for the cases of n = 8, 16, 32 and 40. Similarly, the lower part of Table 2(b) shows the values of ε% between $\omega_{i,\mathrm{FEM}}$ and $\omega_{i,\mathrm{CTMM}}$ ($i = 1-5$). Note that the foregoing values of ε are also obtained from the formula: $\varepsilon = (\omega_{i,X} - \omega_{i,\mathrm{CTMM}}) \times 100\%/\omega_{i,\mathrm{CTMM}}$ with X = LTMM or FEM. From Table 2(b) one sees that, for the case of $n = n_{\min} = 8$, the maximum percentage difference is $\varepsilon_{\max} = 0.196\%$ for ω_3 obtained from LTMM and $\varepsilon_{\max} = 0.062\%$ for ω_5 obtained from FEM. Therefore, for the current example, the solution accuracy of LTMM or FEM is near that of CTMM.

Table 2
Influence of total number of beam segments (n) on the accuracy of the lowest five natural frequencies, ω_v (v = 1–5)

Methods	Total number of beam segments, n	Natural frequencies, ω_v (rad/s)				
		ω_1	ω_2	ω_3	ω_4	ω_5
(a) For the uniform spring-hinged beam carrying an eccentric tip mass and a set of in-span springs as shown in Fig. 3						
LTMM	2	–	73.2035	–	–	–
	4	11.1925	71.6455	240.6655	634.7105	–
		(−0.145%)[a]	(0.530%)	(−0.147%)	(−6.569%)	
	6	11.2015	71.4285	241.0745	673.4885	1146.6905
		(−0.064%)	(0.225%)	(0.022%)	(−0.861%)	(−2.404%)
	8	11.2045	71.3565	241.0735	677.8625	1168.8305
		(−0.037%)	(0.124%)	(0.021%)	(−0.217%)	(−0.519%)
	10	11.2065	71.3245	241.0595	678.8085	1172.9455
		(−0.020%)	(0.080%)	(0.016%)	(−0.078%)	(−0.169%)
	12	11.2070	71.3065	241.0495	679.1035	1174.1055
		(−0.015%)	(0.054%)	(0.012%)	(−0.034%)	(−0.070%)
	14	11.2075	71.2965	241.0425	679.2195	1174.5285
		(−0.011%)	(0.040%)	(0.009%)	(−0.017%)	(−0.034%)
CTMM	2	11.2087	71.2678	241.0210	679.3350	1174.9315
	4	11.2087	71.2678	241.0210	679.3350	1174.9315
FEM	2	22.4584	127.3449	–	–	–
	4	11.2087	71.2702	241.3558	686.9020	1199.2475
		(0.000%)	(0.003%)	(0.139%)	(1.114%)	(2.070%)
	6	11.2087	71.2683	241.0881	681.0135	1183.3461
		(0.000%)	(0.001%)	(0.028%)	(0.247%)	(0.716%)
	8	11.2087	71.2679	241.0423	679.8773	1177.7173
		(0.000%)	(0.000%)	(0.009%)	(0.080%)	(0.237%)
	10	11.2087	71.2678	241.0297	679.5590	1176.0923
		(0.000%)	(0.000%)	(0.004%)	(0.033%)	(0.099%)
	12	11.2087	71.2678	241.0252	679.4435	1175.4963
		(0.000%)	(0.000%)	(0.002%)	(0.016%)	(0.048%)
	14	11.2087	71.2678	241.0232	679.3937	1175.2380
		(0.000%)	(0.000%)	(0.001%)	(0.009%)	(0.026%)
(b) The three-step beam carrying three identical sets of concentrated elements with P– P boundary conditions as shown in Fig. 2 and Case 1 of Table 1						
LTMM	8	57.3661	108.0742	269.4464	281.6303	467.4578
		(0.062%)[a]	(−0.084%)	(0.196%)	(−0.005%)	(0.080%)
	16	57.3392)	108.1404	269.0483	281.6346	467.3561
		(0.016%	(−0.023%)	(0.047%)	(−0.003%)	(0.059%)
	32	57.3325	108.1588	268.9519	281.6400	467.3354
		(0.004%)	(−0.006%)	(0.012%)	(−0.001%)	(0.054%)
	40	57.3317	108.1611	268.9405	281.6438	467.3322
		(0.002%)	(−0.004%)	(0.007%)	(−0.001%)	(0.054%)
CTMM	8	57.3303	108.1652	268.9206	281.6431	467.0818
FEM	8	57.3303	108.1652	268.9240	281.6450	467.3700
		(0.000%)	(0.000%)	(0.001%)	(0.001%)	(0.062%)
	16	57.3303	108.1652	268.9206	281.6435	467.3502
		(0.000%)	(0.000%)	(0.000%)	(0.000%)	(0.057%)
	32	57.3303	108.1651	268.9206	281.6434	467.3490
		(0.000%)	(0.000%)	(0.000%)	(0.000%)	(0.057%)
	40	57.3303	108.1651	268.9206	281.6434	467.3489
		(0.000%)	(0.000%)	(0.000%)	(0.000%)	(0.057%)

[a]The percentage differences obtained from $\varepsilon = (\omega_{i,X} - \omega_{i,\mathrm{CTMM}}) \times 100\% / \omega_{i,\mathrm{CTMM}}$ with X = LTMM or FEM.

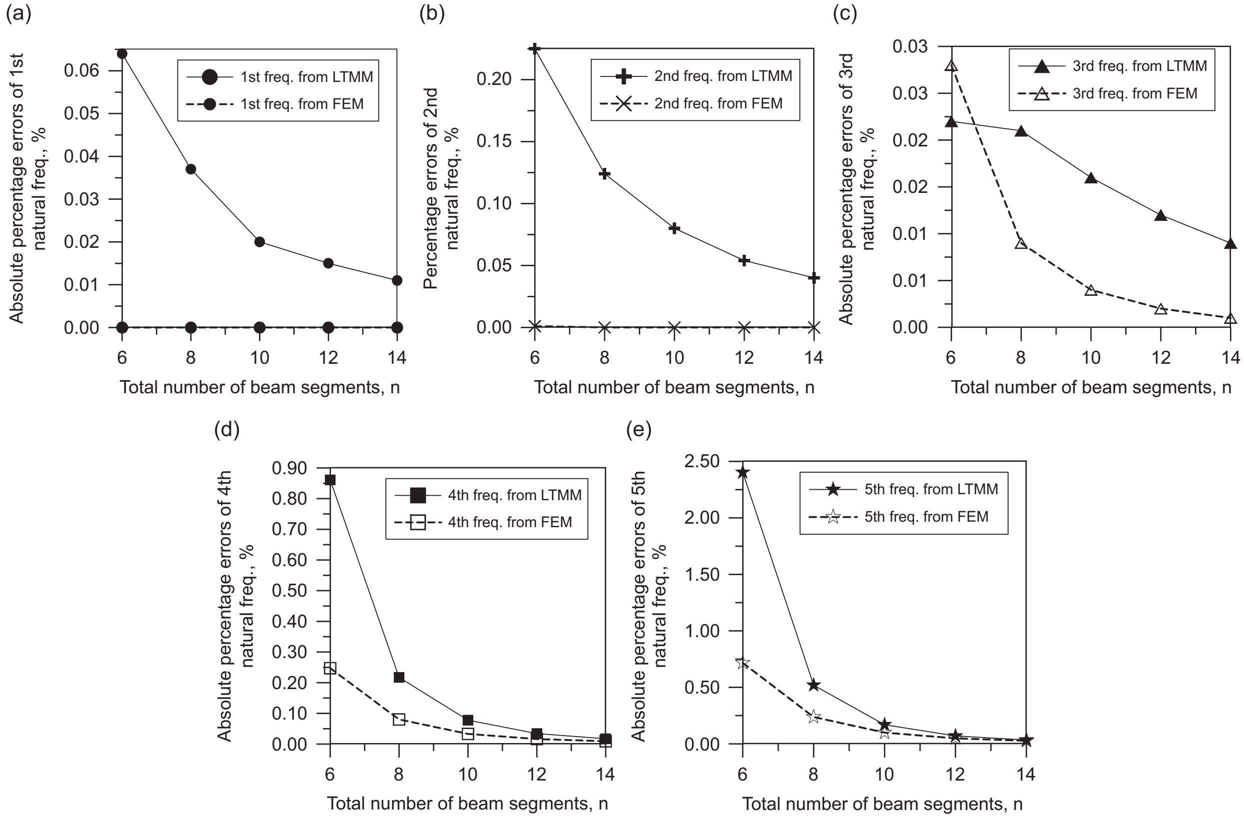

Fig. 4. Influence of total number of beam segments (n) on the ''absolute'' percentage errors ($|\varepsilon|\%$) for the lowest five natural frequencies obtained from LTMM (—●—, —✚—, –▲–, —■— and —★—) and FEM (---○---, ---✖---, ---△---, ---□--- and ---☆---) based on the formula: $|\varepsilon| = |\omega_{i,X} - \omega_{i,\mathrm{CTMM}}| \times 100\%/\omega_{i,\mathrm{CTMM}}$ with $X =$ LTMM or FEM for: (a) ω_1, (b) ω_2, (c) ω_3, (d) ω_4 and (e) ω_5.

5. Conclusions

Comparing with Ref. [25], it is easy to see that the theory of continuous transfer matrix method (CTMM) is much different from that of lumped-mass transfer matrix method (LTMM). This is due to the fact that CTMM is based on the *continuous-mass* model and LTMM is based on the *lumped-mass* model, furthermore, the transfer matrix for an intermediate node in CTMM is to relate the ''integration constants'' for the two adjacent beam segments joined at that node and the transfer matrix for a node (or beam segment) in LTMM is to relate the ''state variables'' (i.e., displacements, slopes, bending moments and shear forces) for the two sides of that node (or beam segment). Therefore, the close agreement between the results of CTMM and those of LTMM should be one of the good evidences that the theories presented and the computer programs developed for CTMM and LTMM are reliable.

In addition to the formulation, the solution convergence of an approximate method is also dependent on the problems tackled. In general, one of the predominant advantages of CTMM superior to LTMM and FEM is its capable of achieving accurate solution by using only a few beam segments, particularly for the cases of a uniform beam carrying a few sets of concentrated elements.

Acknowledgement

The financial support of National Science Council of ROC (NSC95-2221-E-006-493) is much appreciated.

References

[1] M.A. Prohl, A general method for calculating critical speeds of flexible rotors, *Journal of Applied Mechanics* 12 (5) (1945) A-142–A-148.

[2] R.L. Urban, Extension of Holzer–Myklestad–Prohl calculation of turbo-rotor critical speeds, ASME Paper 58-A-246, 1958.

[3] J.W. Lund, Stability and damped critical speeds of a flexible rotor in fluid-film bearings, *Journal of Engineering for Industry* 1 (1974) 509–517.

[4] N.O. Myklestad, A new method of calculating normal modes of uncoupled bending vibration of airplane wings and other types of beams, *Journal of Aeronautical Science* 11 (1944) 153–162.

[5] W.D. Pilkey, P.Y. Chang, *Modern Formulas for Statics and Dynamics*, McGraw-Hill, New York, 1978.

[6] F. Leckie, E. Pestel, Transfer-matrix fundamental, *International Journal of Mechanical Science* 2 (1960) 137–167.

[7] L. Meirovitch, *Analytical Methods in Vibrations*, Macmillan, London, 1967.

[8] C.W. Bert, A.D. Tran, Transient response of a thick beam of bi-modular material, *Earthquake Engineering and Structural Dynamics* 10 (1982) 551–560.

[9] A.D. Tran, C.W. Bert, Bending of thick beams of bi-modulus materials, *Computers & Structures* 15 (6) (1982) 627–642.

[10] J.S. Wu, H.S. Jing, C.C. Cheng, Free vibration analysis of single-layer and two-layer bi-modular beams, *International Journal for Numerical Methods in Engineering* 28 (4) (1989) 955–965.

[11] M.J. Maurizi, R.E. Rossi, J.A. Reyes, Vibration frequencies for a uniform beam with one end spring-hinged and subjected to a translational restraint at the other end, *Journal of Sound and Vibration* 48 (4) (1976) 565–568.

[12] A. Rutenberg, Vibration frequencies for a uniform cantilever with a rotational constraint at a point, *ASME Journal of Applied Mechanics* 45 (1978) 422–423.

[13] K. Takahashi, Eigenvalue problem of a beam with a mass and spring at the end subjected to an axial force, *Journal of Sound and Vibration* 71 (3) (1980) 453–457.

[14] N.G. Stephen, Vibration of a cantilevered beam carrying a tip heavy body by Dunkerley's method, *Journal of Sound and Vibration* 70 (3) (1980) 463–465.

[15] J.H. Lau, Vibration frequencies and mode shapes for a constrained cantilever, *American Society of Mechanical Engineers Journal of Applied Mechanics* 51 (1984) 182–187.

[16] M. Gurgoze, A note on the vibrations of restrained beams and rods with point masses, *Journal of Sound and Vibration* 96 (4) (1984) 461–468.

[17] M. Gurgoze, On the vibrations of restrained beams and rods with heavy masses, *Journal of Sound and Vibration* 100 (4) (1985) 588–589.

[18] W.H. Liu, C.C. Huang, Vibrations of a constrained beam carrying a heavy tip body, *Journal of Sound and Vibration* 123 (1) (1988) 15–29.

[19] R. Firoozian, H. Zhu, A hybrid method for the vibration analysis of rotor-bearing systems, *Proceedings of the Institute of Mechanical Engineers* 205 (Part C) (1991) 131–137.

[20] A.C. Lee, Y. Kang, S.L. Liu, A modified transfer matrix for linear rotor-bearing systems, *Journal of Applied Mechanics, Transactions of the ASME* (1991) 776–783.

[21] O.S. Sener, H.N. Ozguven, Dynamic analysis of geared shaft systems by using a continuous system model, *Journal of Sound and Vibration* 166 (3) (1993) 539–556.

[22] M. Aleyaasin, M. Ebrahimi, R. Whalley, Multivariable hybrid models for rotor-bearing systems, *Journal of Sound and Vibration* 233 (2000) 835–856.

[23] M. Aleyaasin, M. Ebrahimi, R. Whalley, Vibration analysis of distributed-lumped rotor systems, *Computer Methods in Applied Mechanics and Engineering* 189 (2000) 545–558.

[24] C.N. Bapat, C. Bapat, Natural frequencies of a beam with non-classical boundary conditions and concentrated masses, *Journal of Sound and Vibration* 112 (1) (1987) 117–182.

[25] J.S. Wu, C.T. Chen, A lumped-mass TMM for free vibration analysis of a multiple-step beam carrying eccentric tip masses with rotary inertias, *Journal of Sound and Vibration* 301 (2007) 878–897.